# Dual-Mode Filters With Grooved/Splitted Dielectric Resonators for Cellular-Radio Base Stations

Luciano Accatino, *Member, IEEE*, Giorgio Bertin, *Member, IEEE*, Mauro Mongiardo, *Senior Member, IEEE*, and Giuseppe Resnati

***Abstract*—Dual-mode filters for cellular-radio base stations require resonators with a high unloaded $Q$-factor, a wide spurious-free operating window and the possibility of high coupling values either to input or between resonators. These features are obtained by employing a cavity resonator loaded by grooved/splitted ceramic disks, which allows insertion of probes and/or tuning/coupling screws where the field is highly concentrated. In this paper, cavity resonator behavior, intercavity couplings, and filter computer-aided tuning are discussed in detail. Experimental results of an eight-pole transmit filter confirm the suitability of the proposed resonator for realizing cellular-radio base stations filters for UMTS and IMT-2000 applications.**

***Index Terms*—Dielectric resonators, dual-mode filters, modal techniques.**

## I. Introduction

NEXT-GENERATION mobile services will require a large number of cellular-radio base stations with filters specifically developed for UMTS and IMT-2000 applications. Such filters should present favorable characteristics in terms of low losses, appropriate frequency response, miniaturization, and low cost.

In order to reduce dimensions, two techniques, initially developed for satellite applications, are currently adopted: the multiple reuse of the same cavity and the insertion of a low-loss high-permittivity ceramic block within the cavity body [1]–[3].

These techniques have been used in [4] to realize an asymmetric dual-mode filter with conductor-loaded dielectric resonators for the 900-MHz geosynchronous mode (GSM) band. The basic dual-mode cavity there presented makes use of a metal plate placed on top of a ceramic resonator which enlarges the operating bandwidth but reduces the achievable unloaded $Q$. More recently, a dual-mode filter employing dielectric ring resonators with metallic strips has been presented in [5]. In both cases, the conductor losses on the metallic strips deteriorate the cavity $Q$; in addition, such strips or plates once realized are not suitable for tuning.

A different and interesting approach has been proposed in [6] where, instead of placing metallic parts on the dielectric, the resonator shape has been changed in order to achieve quasi-dual-mode resonances while also reducing dimensions. Unfortunately, apart from manufacturing difficulties, the proposed configurations present a lower $Q$ with respect to that achieved by traditional dielectric resonators.

Following the latter approach, we have suggested the use of a grooved ceramic resonator [7], [8]; in some instances, it has been found convenient to extend the groove up to a full air gap, resulting in the splitted resonator configuration examined in more detail in Section II.

The novel dielectric resonator cavity arrangement is presently suggested for realizing a low-loss eight-pole filter for a UMTS-Tx channel. The proposed filter (patent pending) exhibits two different types of intercavity coupling between adjacent cavities; these are discussed in Section III.

The presence of several screws for tuning/coupling purposes makes necessary the use of a sophisticated computer-aided tuning (CAT) procedure. This subject is receiving considerable attention [9]–[11], and a novel automated approach has been suggested in [12]; nonetheless, so far nothing exists for dual-mode filters. A suitable approach, based on the original work of [9], for this type of structure is illustrated in Section IV, where the present filter is also described. Finally, Section V illustrates the measured results of the realized filter with transmission zeros.

## II. Single-Cavity Resonator

### A. Cavity Structure

The proposed cavity resonator is illustrated in Fig. 1; it makes use of a split ceramic resonator, which is simpler to assemby than the grooved one initially proposed in [7] and [8]. As an additional advantage, this arrangement allows the complete insertion of probes and/or screws into areas of high field concentration, providing a much higher coupling/tuning action with respect to the standard single dielectric resonator. Such high values of coupling are typically required in filters used in cellular-radio base stations, where the ratio between useful bandwidths and center frequencies produce relatively large fractional bandwidths, as compared to satellite applications.

Also required for these type of filters are very high values of $Q$. To this end, the high-permittivity resonators are kept in place by using low-permittivity washer-shaped supports. This prevents the direct contact of resonators with conductors, thus reducing ohmic losses and enhancing the unloaded $Q$ values. As illustrated in Table I, a high value of $Q$, in the range of 9000–9500, has been obtained. From the table, it is also apparent that the structure repeateability, when different dielectric samples are considered, is more than satisfactory in terms of $Q$ values and of resonant frequency stability.

Manuscript received April 5, 2002; revised July 29, 2002.

L. Accatino and G. Bertin are with Telecom Italia Lab, 274-10148 Turin, Italy.

M. Mongiardo is with the Dipartimento di Ingegneria Elettronica e delle' Informazione, Università di Perugia, I-06100 Perugia, Italy.

G. Resnati is with FOREM s.r.l., 20041 Agrate Brianza, Italy.

Digital Object Identifier 10.1109/TMTT.2002.805286

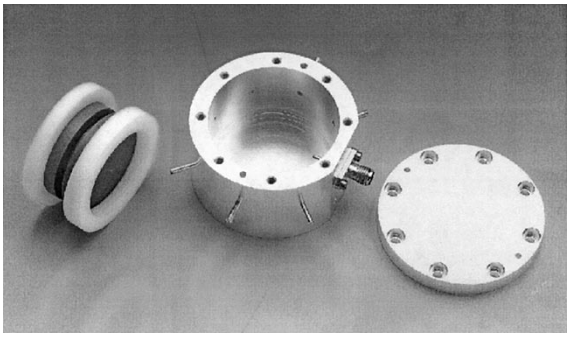

(a)

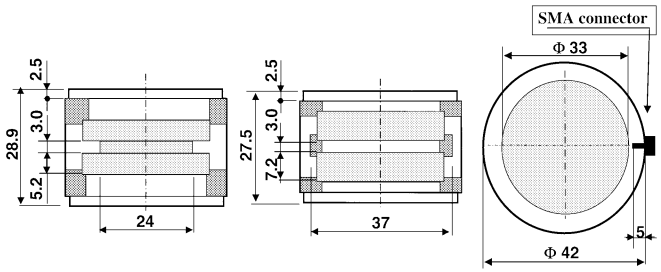


(b)

Fig. 1. (a) Photograph and (b) sketch (side and top views) with dimensions in millimeters of the cavity with the grooved or splitted dielectric resonator. In (b), ceramic resonators are represented in light gray, while washer supports are shown with a darker gray. Note that the groove or the air gap between the ceramic resonators, while not significantly modifying the resonance type, enables the introduction of probes and/or screws into areas of high field concentration.

TABLE I
REPEATABILITY WITH RESPECT TO DIFFERENT CERAMIC RESONATORS. THE TABLE REPORTS MEASURED VALUES OF THE UNLOADED $Q$, RESONANT FREQUENCY, AND FREQUENCY DISTANCE FROM THE FIRST SPURIOUS RESONANCE FOR FIVE DIFFERENT COUPLES OF DIELECTRIC SAMPLES DENOTED AS $a$, $b$, $c$, $d$, AND $e$

| dielectric resonator | unloaded Q | frequency (GHz) | first spurious (MHz) |
|---|---|---|---|
| a | 9575 | 2.255 | +685 |
| b | 9452 | 2.256 | +687 |
| c | 9413 | 2.255 | +687 |
| d | 9340 | 2.257 | +687 |
| e | 9395 | 2.257 | +687 |

### *B. Electromagnetic Analysis*

Analysis, optimization of cavity geometrical dimensions, and evaluation of the unloaded $Q$ are performed at computer level by using an accurate and rigorous full-wave modal routine, based on the approach introduced in [13]. The present analysis method, as illustrated in Fig. 2, takes into account all the relevant geometrical features, apart for screws and coupling probes, including the splitted dielectric resonator geometry, the washer supports with indentations, and the metal housing.

In order to analyze the structure, for each cross section the relative modes are preliminarly found by a transverse resonance approach; then the coupling integrals between the modes of adjacent sections are evaluated and the generalized scattering matrices at the interfaces are obtained. Finally, by connecting together the generalized scattering matrices and by applying the appropriate boundary conditions, one gets the resonant frequencies as zeros of the determinant reported in Fig. 2.

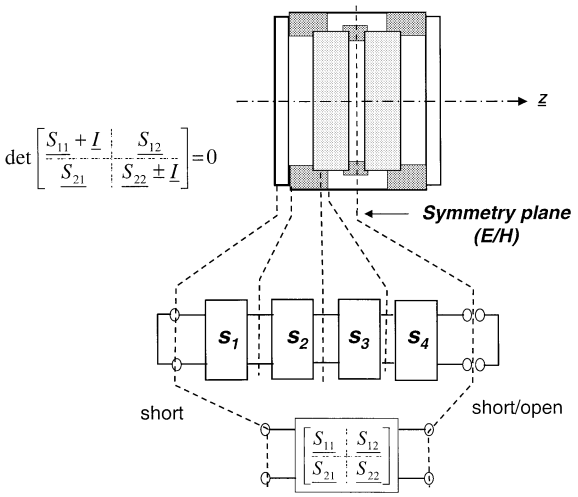


Fig. 2. Modal analysis of the cavity resonances by analyzing the half structure and cascading the generalized scattering matrices.

This dielectric loaded cavity supports hybrid $\mathrm{HE}_{mn}$ resonant modes, where $m$ denotes the angular variation and $n$ is relative to the order of the zero. It may also support $\mathrm{TE}_{0n}$ and $\mathrm{TM}_{0n}$ modes when the angular index $m$ is zero, or when the dielectric filling of the cross section is homogeneous. As the structure is symmetric with respect to the longitudinal axis, all modes display an electric or magnetic wall at symmetry plane and will be denoted, respectively, as $E$ or $H$ type.

The modal spectrum depends on the size and shape of the cavity elements. The resonant mode used for the filter is the dual degenerate $\mathrm{HE}_{11}H$ resonance. The improvement in the spurious-free performance is achieved in two ways: by using symmetries and by optimizing dimensions.

Symmetry is advantageously considered for preventing the excitation of all modes showing an $E$-plane symmetry. This is done by placing the input probe and coupling/tuning elements on the symmetry plane, i.e., in the air gap between the two dielectric disks. Moreover, $\mathrm{TE}_{0n}$ modes are not excited if probes and screws are placed radially.

Theoretical resonances are confirmed by the experimental response also reported in Fig. 3 (middle and lower parts), showing the input reflection coefficient when the cavity is excited by a short straight probe (middle). As can be noted, a wide, spurious-free, operating range is obtained. When a curved probe is used also, unwanted modes are excited (lower).

### *C. Dual-Mode Excitation*

In order to realize the dual-mode excitation in the input cavity, the input probe is placed at a rotated position with respect to reference mode orientation which is determined by the tuning screw position, as illustrated in Fig. 4. This provides the simultaneous coupling of a source node to both resonant modes into the cavity. Coupling between modes, $k_{12}$ in the above figure, is obtained as usual, i.e., by screws placed at 45° with respect to (w.r.t.) to tuning screws. A similar mechanism holds for dual-mode generation in the output cavity. Dual-mode excitations in other cavities (not the input/output ones) are also achieved by placing screws at 45° w.r.t. tuning screws.

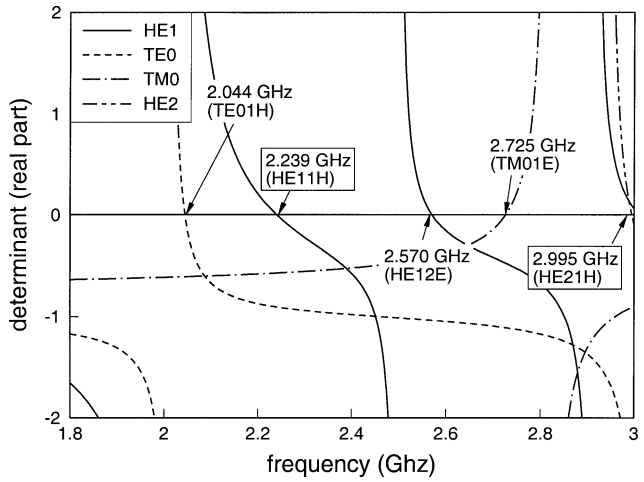


(a)

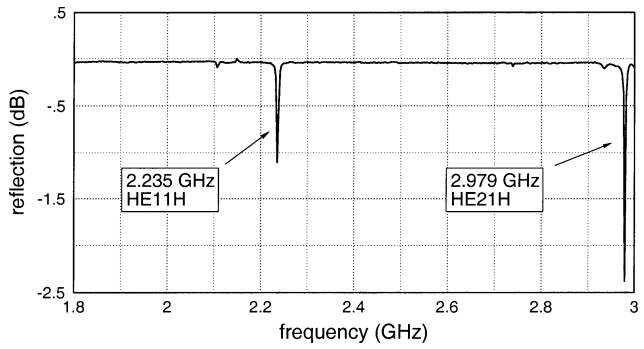


(b)

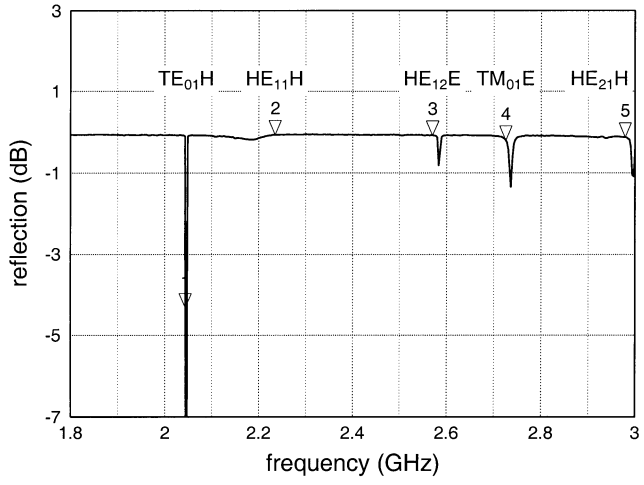


(c)

Fig. 3. (a) Mode chart computed and (b), (c) measured for the cavity with split dielectric resonators. The determinant zeros in the computed chart are the resonant frequencies of all the modes that may exist inside the loaded cavity. When a straigth symmetrical probe is used, modes showing an $E$-plane symmetry are not excited, as shown in (b). (c) A curved probe excites all modes and confirms theorethical results.

### D. Tunability

The single cavity resonator may be tuned in two distinct ways: it is possible to move the top/bottom metallic plate (end-cap tuning) or to adjust the screws inside the cavity. Both effects have been studied and are presented in Fig. 5.

The screw tuning effect is twofold: as the screw is inserted inside the cavity, the resonant frequency becomes lower; however, ohmic losses are also increased, thus causing a $Q$ deterioration, as illustrated in Fig. 5.

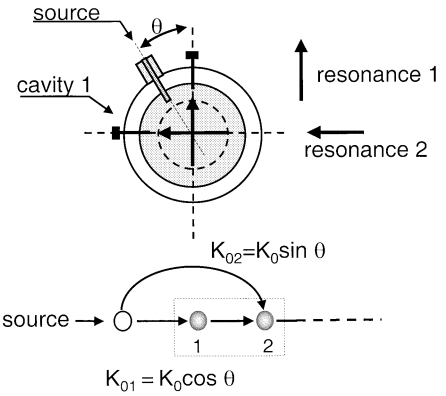


Fig. 4. Realization of the dual mode resonances with a straight probe in the input cavity. Mode resonant frequencies are determined by the tuning screw positions.

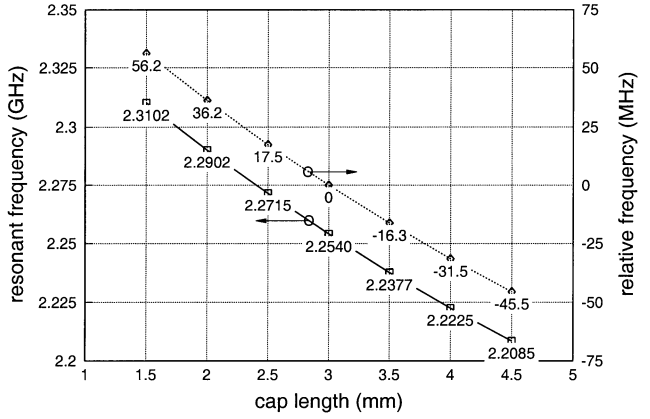


(a)

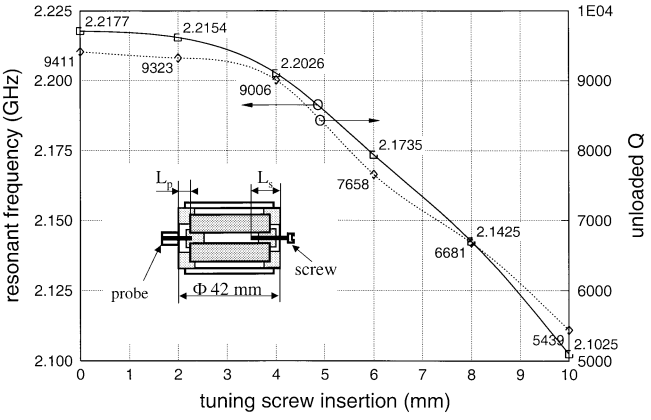


(b)

Fig. 5. Effects of moving: (a) the top plate and (b) tuning screw adjustment.

In order to achieve satisfactory results, it is therefore necessary to first determine the position of the metallic plate; then to adjust the screws for fine tuning, possibly limiting the insertion of the screws to a small extent in order to mantain high values of unloaded $Q$ also for the tuned filter.

## III. Intercavity Coupling

Cavities may be coupled to each other in two ways, as shown in Fig. 6: by placing one on top of the other and using an iris

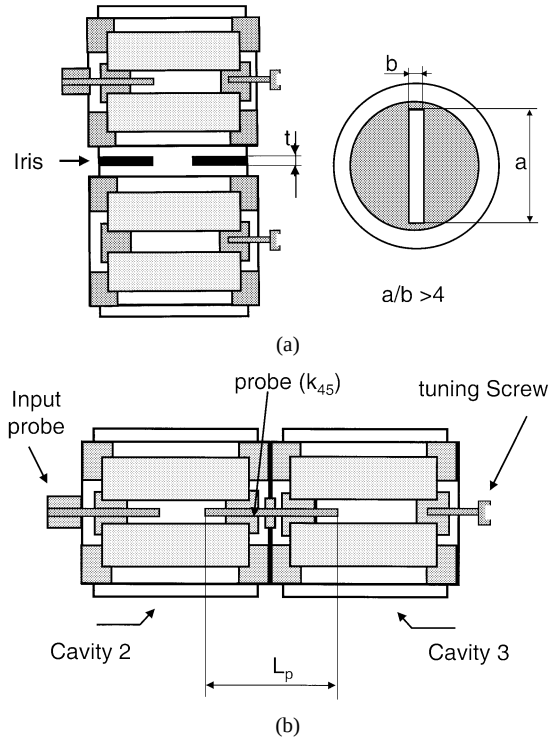


Fig. 6. Intercavity coupling realized: (a) by means of a rectangular iris and (b) by means of an intercavity probe.

coupling or by placing them side by side and considering an intercavity probe as coupling device.

### *A. Iris Coupling*

This type of coupling is realized by using a rectangular iris between the two cavities; typically the ratio between the sidewalls $(a/b)$ is selected in such a way as to allow coupling of only one mode for each cavity.

The network prototype provides the values of coupling, say $k_{ij}$, to be realized. In order to achieve the sought value, the iris geometrical dimensions are determined by using the previously introduced rigorous full-wave model with the inclusion of a further discontinuity representing the iris [14]. Note that, due to symmetry, only half of the structure reported in the upper part of Fig. 6 is analyzed. As an example, for realizing a coupling $k = 0.0222$, an iris width $a = 21.00$ mm has been selected with $b = 2.5$ mm and $t = 2$ mm.

Measurement of the two cavities coupled by the previous iris and tuned to the operating frequency, as illustrated by the two equal dips of the return loss reported in Fig. 7, gives a measured value $k = 0.0226$, showing the reliability of the modal analysis described above.

### *B. Probe Coupling*

Intercavity coupling may also be realized by a probe extending between the splitted resonators; for ease of manufacturing, the intercavity probe diameter is chosen to be the same as the input coupling probe.

An accurate simulation of this type of structure is quite challenging; as a consequence, the correct coupling value (probe length) is achieved experimentally. Both cavities are tuned at

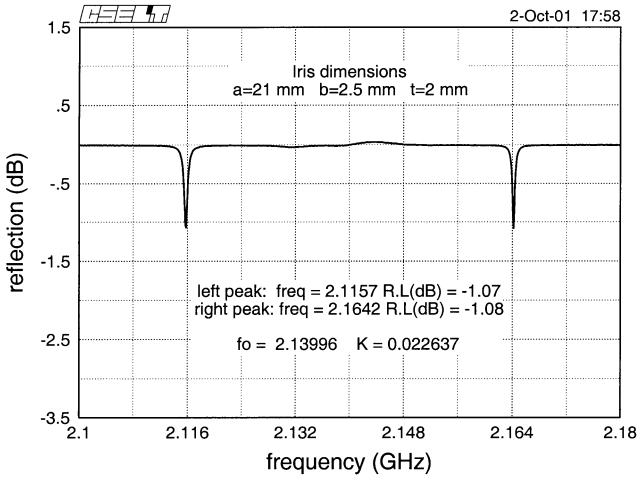


Fig. 7. Measured value of the intercavity coupling realized by means of a rectangular iris.

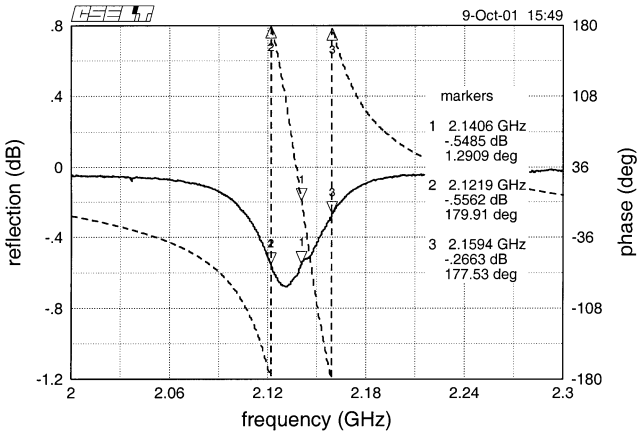


Fig. 8. Measured value of the intercavity coupling realized by means of an intercavity probe.

the resonant frequency by using both the input probe length and the screw present in the second cavity. Fig. 8 reports the measured coupling value in overcoupling conditions.

### *C. Iris and Probe Coupling Properties*

The use of different couplings, either irises or probes, is a way to control the propagation of unwanted modes inside the filter structure. In fact, any $\mathrm{TE}_{01}H$ mode that may accidentally be excited, owing to manufacturing inaccuracies or misalignements, is not coupled to the next cavity either by an end iris or by a central probe. Similarly, the second $\mathrm{HE}_{11}$ resonance $\mathrm{HE}_{11}E$, which is inevitably coupled by an end iris, is not coupled by the central intercavity probe, placed where the (electric) field of the $\mathrm{HE}_{11}E$ mode is zero.

## IV. Computer-Aided Filter Tuning

### *A. Eight-Pole Filter Description*

An eight-pole dual-mode filter has been designed with a center frequency of 2.14 GHz (UMTS transmit frequency) and a bandwidth of 60 MHz. In order to fulfill the filter specifications transmission zeros have been asymmetrically placed on the passband sides at $-1.3$ and 1.4 (normalized low-pass

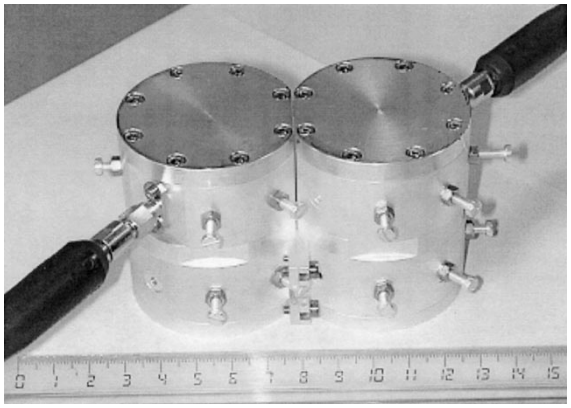

(a)

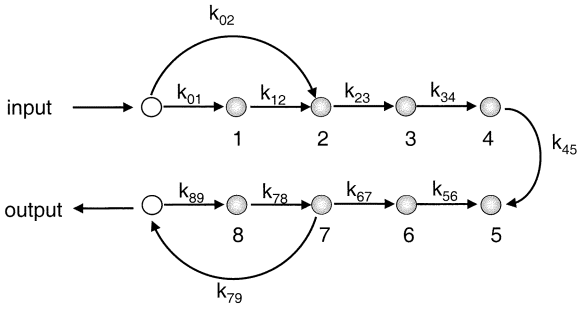


(b)

Fig. 9. Photograph of the eight-pole filter implementing the above routing diagram with input/output trisections.

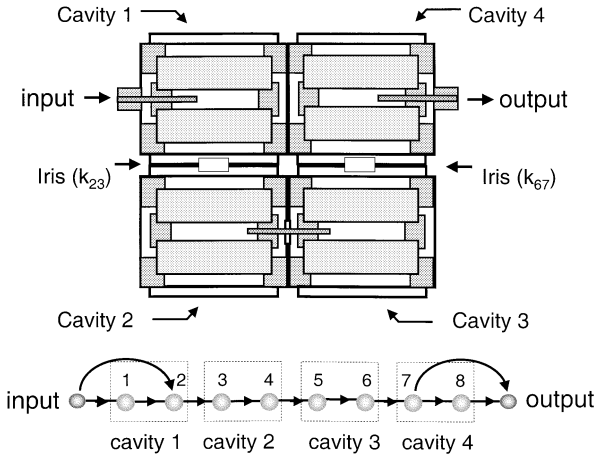


Fig. 10. Eight-pole dual-mode filter structure arrangement (side view). Cavity 1 is connected to cavity 2 by an iris discontinuity; a similar coupling is also used between cavities 3 and 4. The coupling between cavities 2 and 3 is obtained by means of an intercavity probe, visible in the lower part of the figure.

units). Figs. 9–11 illustrate the filter structure and also the routing diagram which shows that the transmission zeros are obtained by using the "trisection" concept [15], with the first trisection placed at the input node and the second at the output node. The proposed cavity arrangement achieves a high degree of compactness and it is useful for preventing propagation of unwanted modes. The structure complexity makes mandatory the use of a CAT procedure for the proper setting of variable elements represented by the screws.

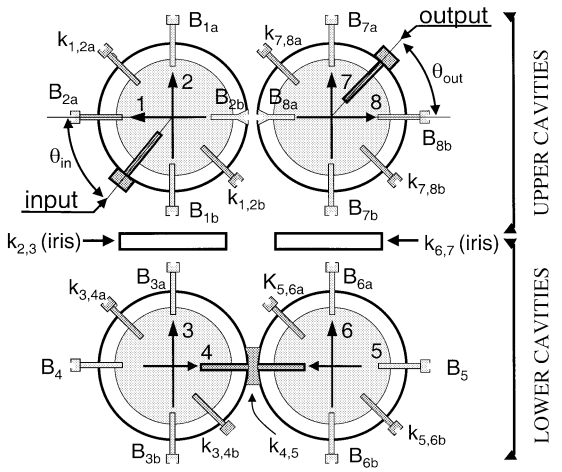


Fig. 11. Eight-pole dual-mode filter: the correspondence between screws and tuning/coupling parameters is illustrated. Note that this represents a first-order approximation, since a particular screw may also affect other network parameters.

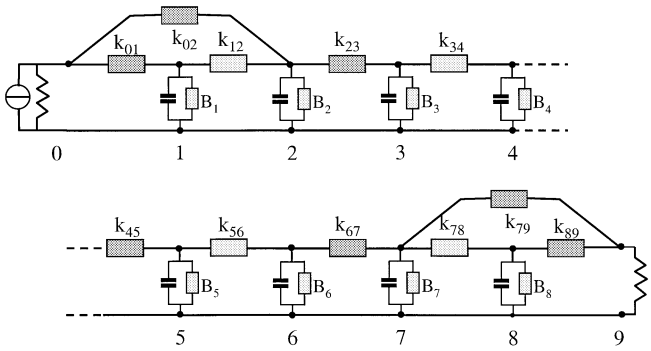


Fig. 12. Normalized network prototype of the eight-pole filter, showing couplings and detunings. Darker "boxes" represent fixed elements; gray boxes denote variable elements.

### *B. CAT: Procedure Description*

We consider a "model" network, which is in fact the normalized network prototype depicted in Fig. 12 and the real filter structure, as reported in Figs. 9 and 10. As discussed in the following, we identify three different sets of parameters: those used to characterize the electrical response, the network prototype parameters, and those related to the actual filter.

The filter electrical response may be efficiently represented in terms of its zero-pole configuration, which is obtained by the input reflection coefficient of the short-circuited network [16]. An example of a short-circuit response is shown in Fig. 13. We will denote with $\mathbf{r}_1$ the vector containing the pole-zero frequency position of the filter measured response; $\mathbf{r}_2$ contains the pole-zero frequency position related to the response of the model network.

Couplings $(k)$ and detuning $(B)$ of the network prototype (see Fig. 11) are collected together in a vector denoted by $\mathbf{K}$, where of course only variable elements are allowed to change in the optimization process described below.

Finally, we denote with $\mathbf{s}$ the vector containing the screw positions; Fig. 11 illustrate the various screws functions in the eight-pole filter.

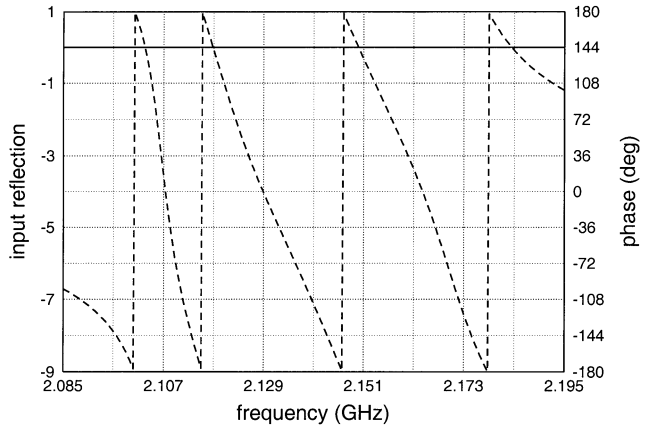


Fig. 13. Phase of the reflection coefficient as computed from the network model with the short-circuited output port. The response is relative to the filter left half section which includes cavities 1 and 2.

The tuning procedure is carried out in an iterative manner and we now describe a typical iteration cycle. For a given filter screw position $\mathbf{s}$, we deduce, *by a measurement process*, the zero-pole values $\mathbf{r}_1 = \mathcal{M}(\mathbf{s})$. The model network is then used to produce a similar result, indicated by $\mathbf{r}_2 = \mathcal{S}(\mathbf{K})$. Now, by using *a fast optimization on the model network*, we find the values of $\mathbf{K}$ which minimize the difference between $\mathbf{r}_1$ and $\mathbf{r}_2$ [9]. In this way, we can associate, with a modest computer effort which does not require any full-wave analysis, a given position of the tuning elements $\mathbf{s}$ to the corresponding network parameters values $\mathbf{K}$ as $\mathbf{K} = \mathcal{F}(\mathcal{M}(\mathbf{s}))$.

On the other hand, from network synthesis, we know the optimal values of the network parameters, denoted by $\mathbf{K}_o$; it is therefore possible to evaluate the distance between the current realization from the optimal one. In order to reduce such a distance, we need to modify the screw positions $\mathbf{s}$.

We note that a phenomenological relationship exists between the network parameters $\mathbf{K}$ and their physical counterpart represented by the tuning screw positions $\mathbf{s}$, as illustrated in Fig. 12. This relationship, although approximate, is used to minimize the distance of the network parameter(s) $\mathbf{K}$ from their optimal value(s) $\mathbf{K}_o$ by a variation of the correspondent filter tuning element(s) $\mathbf{s}$.

The procedure described above, when stated in a more rigorous way, seems to support the validity of the fuzzy logic approach, suggested for the first time in [17], for automated computer-aided filter tuning.

### C. CAT: Application to the Eight-Pole Filter

The complexity induced by the presence of two trisections at the input and output ports suggests dividing the filter into two parts and proceeding to their tuning separately.

The pretuning of two four-pole subnetworks has been made by considering the measurement of the input reflection coefficient, with the output port short-circuited. Fig. 13 shows the same response as computed from the network model.

After application of the short-circuit tuning procedure to the left part of the filter, we obtain the computed (upper) and measured (lower) responses in terms of conventional $S$-parameters

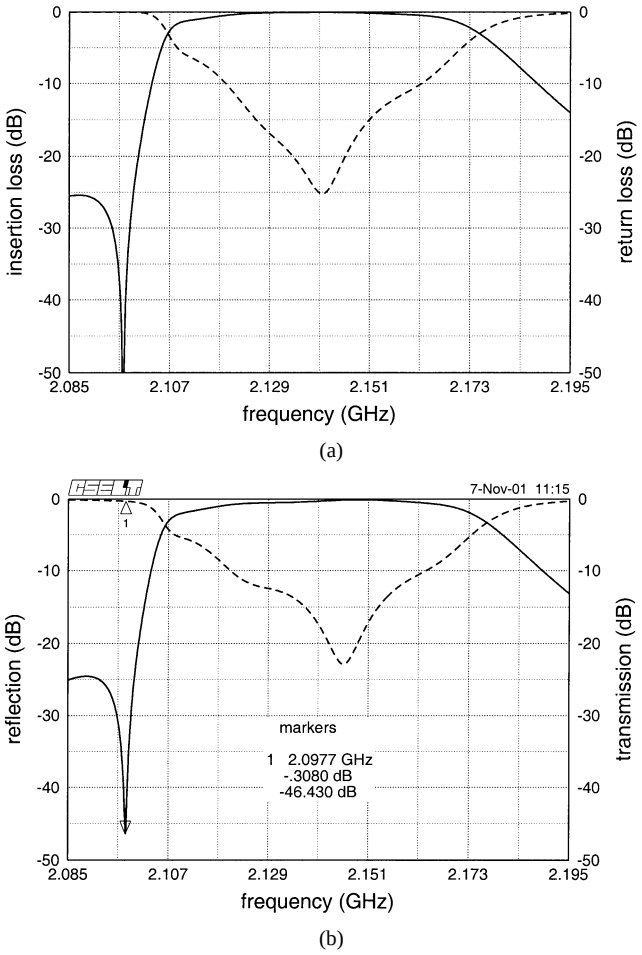


Fig. 14. (a) Measured and (b) computed responses for the left half section.

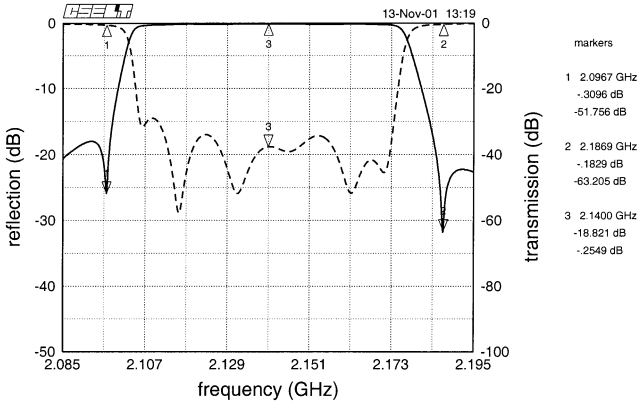


Fig. 15. Measured eight-pole filter response after the two halves have been connected together and before the final tuning.

reported in Fig. 14. The latter figure shows the good degree of correlation that is achieved. A similar approach is also followed for the right part of the filter.

The measured filter response after the two halves have been connected together and are shown before the final tuning in Fig. 15. With a final tuning cycle, mainly performed using the input return loss, we recover the entire filter response shown in Fig. 16.

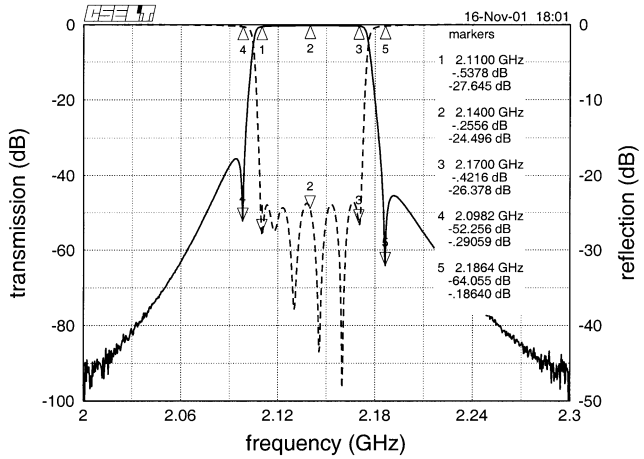


Fig. 16. Measured response of the eight-pole filter.

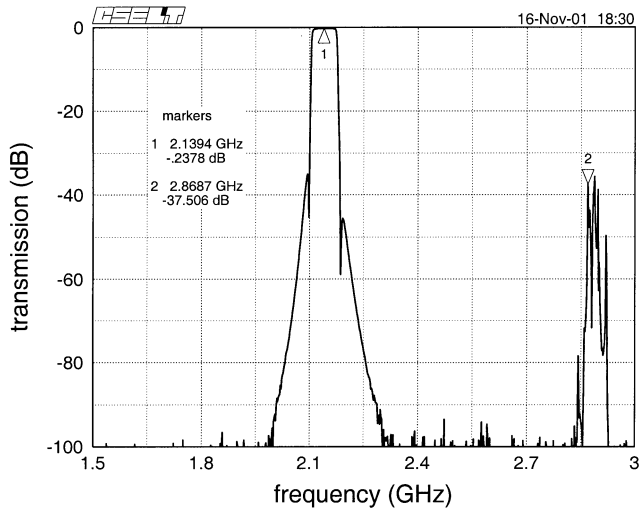


Fig. 17. Measured wide-band response.

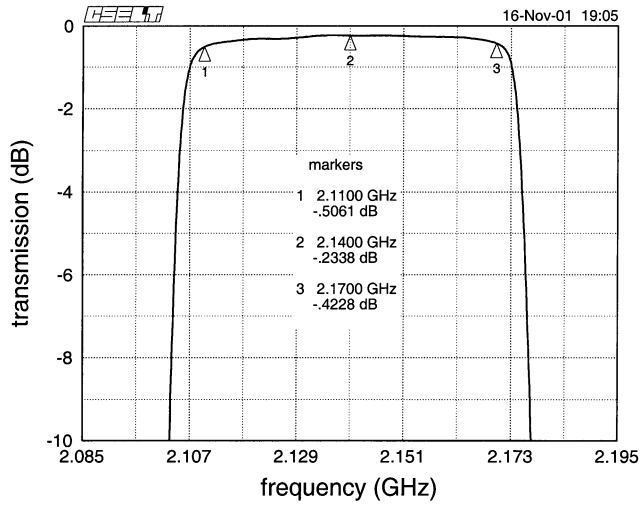


Fig. 18. Measured in-band response.

## V. Results

A prototype filter, with cavities of 27.5-mm height and 42-mm diameter, has been manufactured. The ceramic material has a relative permittivity $\epsilon_r = 34$–$35$ and loss tangent of $5.3 * 10^{-5}$; the supporting washers are made of Teflon, owing to its low permittivity and low loss. The unloaded cavity exibits a resonant frequency of 2.250 GHz with a $Q_u$ of 9000–9500.

The filter measured performance is reported in Figs. 16–18. Low insertion loss ($<$0.3 dB at band center) and a wide spurious-free window ($\sim$700 Mhz) are observed.

## VI. Conclusion

An eight-pole dual-mode filter with transmission zeros, suitable for UMTS or IMT-2000 cellular-radio base station filters, has been realized by using a novel cavity structure with a split dielectric resonator supported by low-permittivity washers.

The proposed configuration exibits high values of coupling and unloaded $Q$ and, by using a specifically developed full-wave simulator, may be optimized for obtaining a sufficiently wide operating frequency window.

Since the filter presents a rather complex tuning arrangement, composed by a large number of screws, a CAT procedure has been introduced. By using the latter, it has been possible to achieve measured results which confirm the structure usefulness for practical applications.

## References

[1] S. J. Fiedziuszko, "Dual-mode dielectric resonator loaded cavity filters," *IEEE Trans. Microwave Theory Tech.*, vol. MTT-30, pp. 1311–1317, Sept. 1982.

[2] L. Accatino, G. Bertin, and M. Mongiardo, "A four-pole dual-mode elliptic filter realized in circular cavity without screws," *IEEE Trans. Microwave Theory Tech.*, vol. 44, pp. 2680–2687, Dec. 1996.

[3] ——, "Elliptical cavity resonators for dual-mode narrowband filters," *IEEE Trans. Microwave Theory Tech.*, vol. 45, pp. 2393–2401, Dec. 1997.

[4] I. C. Hunter, J. D. Rhodes, and V. Dassonville, "Dual mode filters with conductor-loaded dielectric resonators," *IEEE Trans. Microwave Theory Tech.*, vol. 47, pp. 2304–2311, Dec. 1999.

[5] M. Fumagalli, G. Macchiarella, and G. Resnati, "Dual-mode filters for cellular base stations using metallized dielectric resonators," in *IEEE MTT-S Int. Microwave Symp. Dig.*, vol. 3, 2001, pp. 1799–1802.

[6] R. R. Mansour, S. Ye, S. F. Peik, Van Dokas, and B. Fitzpatrick, "Quasidual-mode resonators," *IEEE Trans. Microwave Theory Tech.*, vol. 48, pp. 2476–2481, Dec. 2000.

[7] L. Accatino, G. Bertin, M. Mongiardo, and G. Resnati, "A new dielectric-loaded dual-mode cavity for mobile communications filters," in *Proc. 31th Eur. Microwave Conf.*, vol. 1, London, U.K., 2001, pp. 37–40.

[8] ——, "Dual-mode filters with grooved dielectric resonators for cellular-radio base stations," in *IEEE MTT-S Int. Microwave Symp. Dig.*, vol. 3, 2002, pp. 1453–1456.

[9] L. Accatino, "Computer-aided tuning of microwave filters," in *IEEE MTT-S Int. Microwave Symp. Dig.*, 1986, pp. 249–252.

[10] J. Dunsmore, "Tuning band pass filters in the time domain," in *IEEE MTT-S Int. Microwave Symp. Dig.*, 1999, pp. 1351–1354.

[11] A. E. Atia and H.-W. Yao, "Tuning and measurements of couplings and resonant frequencies for cascaded resonators," in *IEEE MTT-S Int. Microwave Symp. Dig.*, vol. 3, 2000, pp. 1637–1640.

[12] P. Harscher and R. Vahldieck, "Automated computer controlled tuning of waveguide filters using adaptive network models," *IEEE Trans. Microwave Theory Tech.*, vol. 49, pp. 2125–2130, Nov. 2001.

[13] K. A. Zaki and C. Chen, "New results in dielectric-loaded resonators," *IEEE Trans. Microwave Theory Tech.*, vol. 34, pp. 815–824, July 1986.

[14] L. Accatino and G. Bertin, "Design of coupling irises between circular cavities by modal analysis," *IEEE Trans. Microwave Theory Tech.*, vol. 42, pp. 1307–1313, July 1994.

[15] R. J. Cameron, "General prototype network-synthesis methods for microwave filters," *ESA J.*, vol. 6, pp. 193–206, 1982.

[16] A. E. Atia and A. E. Williams, "Measurements of intercavity couplings," *IEEE Trans. Microwave Theory Tech.*, vol. MTT-23, pp. 519–522, June 1975.

[17] R. R. Mansour, "Filter computer-aided tuning by a fuzzy logic approach," unpublished.

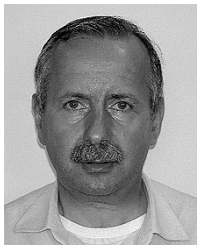

**Luciano Accatino** (M'84) was born in Turin, Italy, in 1950. He received the Laurea degree in electronic engineering from the Polytechnic School of Turin, Turin, Italy, in 1973.

In 1975, he joined the Microwave Department, Centro Studie Laboratorie Telecommunicazioni S.p.A. (CSELT) [now the Telecom Italia Lab (TILAB)], Turin, Italy, where he was initially engaged in the design of microstrip circuits and components. In 1980, he became involved in the design and development of microwave cavity filters and, subsequently, of various components for beam-forming networks. He then supervised the activities related to filters and waveguide components at CSELT, stimulating a wide application of electromagnetic models to the design of all passive components.

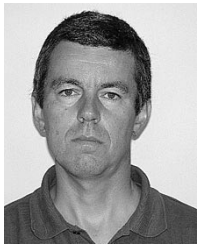

**Giorgio Bertin** (M'92) was born in Aosta, Italy, in 1956. He received the Laurea degree in electronic engineering from the Polytechnic School of Turin, Turin, Italy, in 1982.

In 1983, he joined the Microwave Department of Centro Studie Laboratorie Telecommunicazioni S.p.A. (CSELT) [now the Telecom Italia Lab (TILAB)], Turin, Italy, where he was first engaged in dielectric oscillator and dielectric-loaded cavity design. His activities then focused on the modeling of microwave discontinuities and the computer-aided design of guiding structures, with particular attention devoted to discontinuities between nonstandard waveguides, such as those involving a dielectric loading or the presence of ridges. His current interests include multimode dielectric-resonator filters and antenna components design.

**Mauro Mongiardo** (M'91–SM'00) received the Laurea degree (*summa cum laude*) from the University of Rome, Rome, Italy, in 1983, and the Ph.D. degree from the University of Bath, Bath, U.K., in 1991.

From 1983 to 1991, he was a Research Associate and then Assistant Professor at the University of Rome "Tor Vergata," Rome, Italy. In 1991, he was Associate Professor at the University of Palermo, Palermo, Italy. In 1992, he joined the Università di Perugia, Perugia, Italy, as an Associate. Since 2001, he has been a Full Professor with the Dipartimento di Ingegneria Elettronica e delle' Informazione (DIEI), Università di Perugia. He has been a Visiting Scientist at the University of Victoria, Victoria, BC, Canada, the University of Bath, Bath, U.K., Oregon State University, Corvallis, and the Technical University of Munich, Munich, Germany. His research interests include numerical methods to model electromagnetic (EM) fields, particularly for computer-aided design (CAD) of microwave and millimeter-wave passive components. He is also interested in the development of new designs for microwave components and filters. His main contributions have been in the areas of modal analysis, integral equations, finite difference time domain (FDTD), transmission line matrix (TLM), finite-element method (FEM), and hybrid methods.

Dr. Mongiardo has served on the Technical Program Committee of the IEEE Microwave Theory and Techniques Society (IEEE MTT-S) International Microwave Symposium (IMS) since 1992. Since 1994, he has been an Editorial Board member for the IEEE TRANSACTIONS ON MICROWAVE THEORY AND TECHNIQUES. He is also a member of the IEEE MTT-S Technical Program Committee (TPC) on CAD and has served as reviewer for the European Microwave Conference.

**Giuseppe Resnati** was born in Seregno, Italy, in 1962. He received the Dr. degree in physics from the University of Milan, Milan, Italy, in 1988.

In 1992, he joined FOREM s.r.l., Agate Brianza, Italy, as an RF Engineer, where he was involved in the design and simulation of passive devices, filters in waveguides, and coaxial and dielectric technologies. He is currently Director of the Research and Development Department, FOREM s.r.l.